JACS
JOURNAL OF THE AMERICAN CHEMICAL SOCIETY

COMMUNICATION

pubs.acs.org/JACS

Plasmonic Enhancements of Photocatalytic Activity of Pt/n-Si/Ag Photodiodes Using Au/Ag Core/Shell Nanorods

Yongquan Qu,[†] Rui Cheng,[‡] Qiao Su,[†] and Xiangfeng Duan*[,†,§]

[†]Department of Chemistry and Biochemistry, [‡]Department of Materials Science and Engineering, and [§]California NanoSystems Institute, University of California, Los Angeles, California 90095, United States

Supporting Information

ABSTRACT: We report the plasmonic enhancement of the photocatalytic properties of Pt/n-Si/Ag photodiode photocatalysts using Au/Ag core/shell nanorods. We show that Au/Ag core/shell nanorods can be synthesized with tunable plasmon resonance frequencies and then conjugated onto Pt/n-Si/Ag photodiodes using well-defined chemistry. Photocatalytic studies showed that the conjugation with Au/Ag core/shell nanorods can significantly enhance the photocatalytic activity by more than a factor of 3. Spectral dependence studies further revealed that the photocatalytic enhancement is strongly correlated with the plasmonic absorption spectra of the Au/Ag core/shell nanorods, unambiguously demonstrating the plasmonic enhancement effect.

Photocatalytsts can harness solar energy to drive useful redox chemistry and therefore are of considerable interest for solar energy harvesting, conversion, and storage as well as environmental pollutant treatment.[1] We recently reported the design and synthesis of a new generation of photocatalysts involving integration of a nanoscale photodiode with two distinct redox nanocatalysts in a single nanowire heterostructure.[2,3] Specifically, a nanoscale metal/semiconductor (e.g., Pt/n-Si) Schottky diode is encased in a protective insulating shell (silicon oxide) and integrated with two metallic nanocatalysts (e.g., Pt and Ag) in a heterojunction nanowire. The internal built-in potential across the Schottky diode promotes the efficient dissociation of photoexcited electron−hole pairs and directs the transport of the separated charge carriers to the integrated redox catalysts for improved photocatalytic activity. The silicon oxide shell also prevents direct electrochemical reactions on the semiconductor surface and therefore ensures exceptional photochemical stability.

This rational design of photocatalytic nanosystems allows efficient charge separation, transport, and utilization to enable excellent photocatalytic quantum efficiency. However, the overall efficiency of the Pt/n-Si/Ag photodiodes can still be limited by relatively low optical absorption (<20%).[2,3] Here we report a further enhancement of the photocatalytic performance of such photodiodes using Au and Au/Ag core/shell plasmonic nanorods. Coupling plasmonic metal nanostructures with semiconductor materials has the potential to increase significantly the absorption of semiconductors through a local field enhancement effect.[4,5] However, the investigation of plasmonic-enhanced photocatalytic properties is less straightforward. Most studies carried out to date have involved direct contact between the metallic nanostructures and the semiconductors.[4] With this direct coupling, the enhanced photoactivity is often convoluted and has been attributed to the roles of the metal nanostructures as the electron-trapping centers and/or the local surface plasmon resonance effect.[4] It is often difficult to differentiate these two fundamentally different mechanisms. On the other hand, direct contact between the metal and the semiconductor may also introduce interface trapping states that can increase electron−hole recombination and Fermi level pinning to degrade the photocatalytic activity.[5c,6] Indeed, a reduced photocatalytic activity has also recently been reported for photocatalysts with direct contact between the metal nanostructures and the semiconductor materials.[5] Introducing a thin insulating shell to provide electrical isolatation of the metal nanostructures can avoid the interface defects and/or charge transfer between the semiconductor and the metal while allowing the propagation of an optical field around the metal nanostructures, resulting in locally concentrated light for the enhancement of photocatalytic activity.[7]

Herein we report an unambiguous investigation of plasmonic modulation of photocatalyst properties by coupling plasmonic nanostructures (Au nanorods and Au/Ag core/shell nanorods) and Pt/n-Si/Ag photodiode photocatalysts with ∼15 nm thick silicon oxide shells. The Au/Ag core/shell nanorods were selected here because of their broad plasmon resonance tunability from the near-UV to the IR range, which allows for wide spectral dependence studies. The 15 nm silicon oxide shell can serve several purposes: (1) It protects the semiconductor materials from direct photoelectrochemical corrosion to improve the stability; without this protection, the photoelectrochemical corrosion could lead to degradation/dissolution of the semiconductors and/or cause the metal nanostructures to break away from the semiconductors. (2) It avoids direct charge exchange between the semiconductor and the metal to avoid the formation of interface defects and Fermi level pinning. (3) It prevents the metal nanostructures from functioning as an additional cocatalyst for photocatalytic reactions that could complicate the interpretation of the results. Therefore, the coupling of silicon oxide-insulated Pt/n-Si/Ag photodiodes with Au/Ag nanorods provides an interesting and clean system for investigating the plasmonic effect on photocatalysis.

Received: May 12, 2011
Published: October 03, 2011

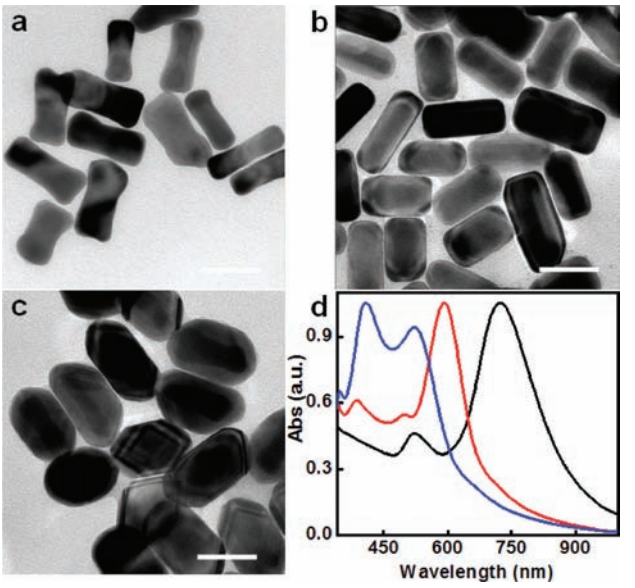

Figure 1. Structure and spectroscopic characterization of Au and Au/Ag core/shell nanorods. (a−c) TEM images of (a) Au nanorods, (b) Au/Ag core/shell nanorods-A with a Ag/Au molar ratio of 0.86, and (c) Au/Ag core/shell nanorods-B with a Ag/Au molar ratio of 2.58. The scale bars in (a−c) are all 50 nm. (d) Absorption spectra of the Au and Au/Ag core/shell nanorods shown in (a−c): black, Au nanorods; red, Au/Ag core/shell nanorods-A; blue, Au/Ag core/shell nanorods-B.

The Au/Ag core/shell nanorods were synthesized by adding gold nanorod seeds (Figure 1a) into a silver coating solution containing silver nitrate ($AgNO_3$), ascorbic acid (AA), and sodium hydroxide (NaOH).[8] For a fixed amount of gold nanorod seeds, increasing the amount of $AgNO_3$ led to a strong color change from light-brown to green, orange, and yellow, suggesting a change of plasmonic absorption due to the formation of the silver coating. Transmission electron microscopy (TEM) studies clearly showed Au/Ag core/shell nanorod structures (Figure 1b,c). The images also confirmed the expected increase of silver shell thickness with increasing concentration of $AgNO_3$ in the coating solution. UV−vis absorption spectroscopic studies clearly showed the obvious tunability of the spectral features. With increasing silver ion concentration and consequently increasing silver shell thickness, the resulting plasmonic absorption peaks were progressively blue-shifted relative to the spectrum of the starting gold nanorods (Figure 1d).

The synthetic method for the Pt/n-Si/Ag nanowire photodiodes is summarized in our previous report[3] and the Supporting Information (SI). In brief, the silicon nanowire arrays were prepared by electroless wet chemical etching followed by baking at 900 °C under ambient conditions to form a silicon oxide shell with a thickness of ~15 nm. The Pt/Si heterojunction nanowires were prepared through partial silicon dry etching followed by electrodeposition of Pt. Silver metal was deposited on the silicon end of Pt/Si heterojunction nanowires through a self-catalyzed photoreduction process. The TEM image in Figure 2a clearly shows the interface of the Pt/Si heterostructure with a silver particle anchored at the silicon end of the nanowire. Energy-dispersive X-ray (EDX) studies further confirmed the three distinct sections of Pt, Si, and Ag in the heterojunction nanowire.

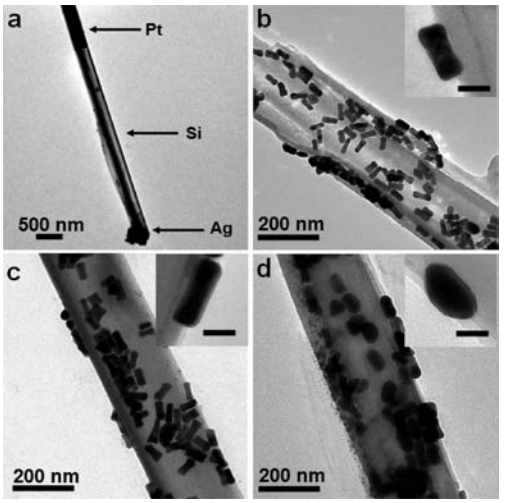

Figure 2. TEM images of (a) a Pt/n-Si/Ag photodiode, (b) a photodiode photocatalyst with Au nanorods loaded on the surface, (c) a photodiode photocatalyst with Au/Ag core/shell nanorods-A on the surface, and (d) a photodiode photocatalyst with Au/Ag core/shell nanorods-B on the surface. The insets in (b−d) show images of individual nanorods on the surfaces of the photodiodes. The scale bars in the insets are 30 nm.

The three kinds of Au or Au/Ag plasmonic nanorods were then loaded on the surfaces of photodiodes using (3-mercaptopropyl)trimethoxysilane (MPTMS) as the coupling agent. To this end, MPTMS was first used to modify the Au and Au/Ag core/shell nanorods. The silane-modified nanorods were then conjugated onto the silicon oxide shell of the photodiodes in ethanol solution. Coupling the photodiodes with Au nanorods (Figure 1a), Au/Ag core/shell nanorods-A (Figure 1b), and Au/Ag core/shell nanorods-B (Figure 1c) afforded three photocatalysts, named as Au NRs−Diodes (Figure 2b), Au/Ag NRs-A−Diodes (Figure 2c), and Au/Ag NRs-B−Diodes (Figure 2d), respectively. The average number of metallic nanorods per micrometer length of photodiode nanowire was about 200, 175, and 115 for AuNRs, Au/Ag core/shell nanorods-A, and Au/Ag core/shell nanorods-B, respectively.

The photocatalytic degradation of organic dyes or toxic pollutants is of great significance in environmental pollutant treatment and represents a commonly used approach to characterize the activity of photocatalysts. To this end, photocatalytic degradation of nitrobenzene (NB) was performed to evaluate the photocatalytic activity of the photodiodes and plasmonic resonance effect of the metal nanorods. NB has an absorption peak at 267 nm (Figure S1 in the SI) that does not interfere with the light absorption of the plasmonic nanostructures. For photocatalytic studies, photocatalysts containing 2 mg of photodiodes were dispersed in 10 mL of 300 μM NB aqueous solution. The reaction mixtures were exposed to light irradiation from a 300 W xenon lamp (power density ~0.56 W/cm^2) under vigorous stirring. The experimental parameters were identical for all reactions. The reaction system was cooled by air flow. Small aliquots were taken out at different reaction times. The nanowire photodiodes were centrifuged off, and the concentration of the NB aqueous solution was monitored by UV−vis absorption spectroscopy.

Figure 3a shows the concentration of the NB solution as a function of reaction time. The blue up-triangles, red circles, olive diamonds, and purple right-triangles represent the NB dye

dx.doi.org/10.1021/ja204383q |J. Am. Chem. Soc. 2011, 133, 16730–16733

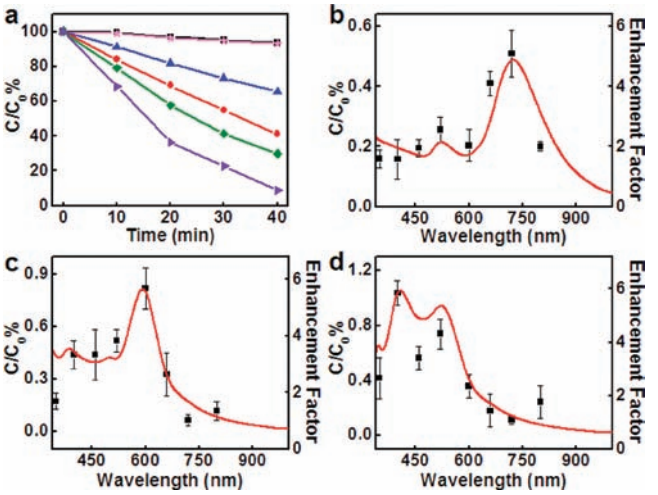

Figure 3. (a) Photocatalytic activities of two controls and four catalysts in the NB degradation reaction: NB alone (black squares); mixture of NB and Au/Ag core/shell nanorods-B (magenta stars); Pt/n-Si/Ag photodiodes alone (blue triangles); Au NRs−Diodes (red circles); Au/Ag NRs-A−Diodes (olive diamonds); Au/Ag NRs-B−Diodes (violet right-triangles). (b) Photoactivity enhancement factor (black squares) for Au NRs−Diodes as a function of excitation wavelength. The solid curve is the absorption spectrum of Au nanorods. (c) Photoactivity enhancement factor (black squares) for Au/Ag NRs-A−Diodes as a function of excitation wavelength. The solid curve is the absorption spectrum of Au/Ag core/shell nanorods. (d) Photoactivity enhancement factor (black squares) for Au/Ag NRs-B−Diodes as a function of excitation wavelength. The solid curve is the absorption spectrum of Au/Ag core/shell nanorods.

photodegradation catalyzed by photodiodes, Au NRs−Diodes, Au/Ag NRs-A−Diodes and Au/Ag NRs-B−Diodes, respectively. The percentage of NB degraded by pure photodiodes was 34.6% within 40 min of light irradiation. In contrast, light irradiation of NB alone and of a mixture of NB and 1 mg of Au/Ag core/shell nanorods-B resulted in slow photodegradation of NB (~7% within 40 min), confirming that the photocatalytic activity indeed originated from the Pt/Si/Ag photodiodes. Significantly larger percentages of NB were degraded with the Au NRs−Diodes, Au/Ag NRs-A−Diodes, and Au/Ag NRs-B−Diodes. The apparent photodegradation rates of NB catalyzed by these materials during the first 20 min linear degradation region were respectively 1.61, 2.20, and 3.30 times that of the reaction catalyzed by photodiodes alone. The experiments were repeated three times to confirm the plasmonic enhancement effect. Compared with photodiodes alone, the average enhancement factors were 1.68 ± 0.08, 2.09 ± 0.09, and 3.18 ± 0.11 for Au NRs−Diodes, Au/Ag NRs-A−Diodes, and Au/Ag NRs-B−Diodes, respectively. Because of the existence of the silicon oxide shell on the surface of the photodiodes, the accelerated rate of NB photodegradation is not a result of metal nanorods acting as electron traps to aid electron−hole separation or an additional cocatalytic effect by the metal nanostructures. It can therefore be attributed to the plasmonic resonance effect of the metal nanostructures.

To provide further confirmation that the enhancement was due to the plasmonic resonance effect, we investigated the spectral dependence of the photocatalytic activity. In this case, a monochromator (Corner 260, Newport) was used to modulate the wavelength of the incident light. All of the experiments were repeated three times to ensure consistency between experiments. Figure 3b shows the photoactivity enhancement factor for the Au NRs−Diode composites relative to that of the photodiodes alone as a function of the irradiation wavelength. The results clearly demonstrate that the enhancement shows a strong spectral dependence that qualitatively matches well with the intensity of the UV−vis extinction spectrum of the Au nanorods. The same phenomenon was also observed for Au/Ag NRs-A−Diodes and Au/Ag NRs-B−Diodes (Figure 3c,d). Since gold or silver extinction is a consequence of the excitation of the local surface plasmon resonance, the qualitative match between the metal nanorods' plasmon resonance intensities and the corresponding enhancement factors unambiguously demonstrates that the plasmon resonance of the metal nanorods is the primary factor responsible for the enhanced photocatalytic activity of the photodiodes. Parallel studies on photodegradation of indigo carmine (IC) also showed qualitatively similar results (Figure S2), further confirming the strong plasmonic enhancement of the photoactivity of the Pt/Si/Ag photodiodes.

We also used the finite-difference time-domain (FDTD) approach to simulate the plasmon resonance enhancement of the local optical field. The simulation showed that an optical field enhancement of more than 1 order of magnitude can be achieved in the very proximity of the plasmonic nanostructures and that the enhancement quickly decays to a much smaller enhacement factor of 1.5−5 at a distance of 15 nm from the plasmonic nanostructures (Figure S3). The overall enhancement factors observed in our experiment are comparable to or slightly better than the simulation results. A few factors may contribute to the additional enhancement. First, the existence of aggregated plasmonic nanorods and the local field coupling between the plasmonic nanorods could increase the enhancement depth. Second, the enhancement within the 15 nm SiO_2 could also contribute to the overall enhancement of absorption through an optical trapping effect (i.e., the photon can be trapped within the nanowires by means of a wave-guiding effect).[9]

In summary, we have designed and synthesized a model system to provide a definitive investigation of plasmonic-resonanace-enhanced photocatalytic properties by coupling Pt/n-Si/Ag photodiodes with Au nanorods or Au/Ag core/shell nanorods. Our studies have shown that the local surface plasmon resonance of metal nanostructures can be employed to enhance light absorption of semiconductor materials, resulting in greatly enhanced photoactivity. The overlap between the UV−vis absorption of the metal nanorods and the spectral-dependent enhancement factor for each photocatalyst demonstrates strongly that the enhanced photoactivity can be attributed the local surface plasmon resonance of the metal nanorods. It is well-known that the plasmonic enhancement effect is highly localized to the surface of metal nanostructures with a roughly exponentially decay of the strength in space (Figure S3).[7] With the continued optimization of the heterostructures (e.g., by reducing the oxide layer thickness), it should be possible to improve the enhancement effect further.

■ ASSOCIATED CONTENT

Supporting Information. Experimental details about synthesis of nanostructures and photocatalytic reactions. This material is available free of charge via the Internet at http://pubs.acs.org.

AUTHOR INFORMATION

Corresponding Author
xduan@chem.ucla.edu

ACKNOWLEDGMENT

We acknowledge support by the NIH Director's New Innovator Award Program, part of the NIH Roadmap for Medical Research, through Grant 1DP2OD004342-01. We acknowledge the Electron Imaging Center for Nanomachines (EICN) at UCLA for support for TEM.

REFERENCES

(1) (a) Hagfeldt, A.; Grätzel, M. *Acc. Chem. Res.* **2000**, *33*, 269. (b) Gomez-Romero, P. *Adv. Mater.* **2001**, *13*, 163. (c) Goetzberger, A.; Hebling, C.; Schock, H. W. *Mater. Sci. Eng., R* **2003**, *40*, 1. (d) Lewis, N. S. *Science* **2007**, *315*, 798. (e) Tian, B.; Kempa, T. J.; Lieber, C. M. *Chem. Soc. Rev.* **2009**, *38*, 16. (f) Law, M.; Greene, L. E.; Johnson, J. C.; Saykally, R.; Yang, P. D. *Nat. Mater.* **2005**, *4*, 455. (g) Tian, B. Z.; Zheng, X. L.; Kempa, T. J.; Fang, Y.; Yu, N. F.; Yu, G. H.; Huang, J. L.; Lieber, C. M. *Nature* **2007**, *449*, 885. (h) Qu, Y. Q.; Liao, L.; Li, Y. J.; Zhang, H.; Huang, Y.; Duan, X. F. *Nano Lett.* **2009**, *9*, 4539. (i) Qu, Y. Q.; Zhong, X.; Li, Y. J.; Liao, L.; Huang, Y.; Duan, X. F. *J. Mater. Chem.* **2010**, *20*, 3590. (j) Xu, S.; Qin, Y.; Xu, C.; Wei, Y. G.; Yang, R. S.; Wang, Z. L. *Nat. Nanotechnol.* **2010**, *5*, 366. (k) Wang, Z. L. *Nano Today* **2010**, *5*, 540. (l) Li, J. H.; Zhang, J. Z. *Coord. Chem. Rev.* **2009**, *253*, 3015.

(2) Qu, Y. Q.; Liao, L.; Cheng, R.; Wang, Y.; Lin, Y. C.; Huang, Y.; Duan, X. F. *Nano Lett.* **2010**, *10*, 1941.

(3) Qu, Y. Q.; Xue, T.; Zhong, X.; Lin, Y. C.; Liao, L.; Choi, J. N.; Duan, X. F. *Adv. Funct. Mater.* **2010**, *20*, 3005.

(4) (a) Chandrasekharan, N.; Kamat, P. V. *J. Phys. Chem. B* **2000**, *104*, 10851. (b) Jakob, M.; Levanon, H.; Kamat, P. V. *Nano Lett.* **2003**, *3*, 353. (c) Subramanian, V.; Wolf, E. E.; Kamat, P. V. *J. Am. Chem. Soc.* **2004**, *126*, 4943. (d) Hirakawa, T.; Kamat, P. V. *Langmuir* **2004**, *20*, 5645. (e) Kamat, P. V. *J. Phys. Chem. C* **2008**, *112*, 18737. (f) Hirakawa, T.; Kamat, P. V. *J. Am. Chem. Soc.* **2005**, *127*, 3928. (g) Wu, X. F.; Song, H. Y.; Yoon, J. M.; Yu, Y. T.; Chen, Y. F. *Langmuir* **2009**, *25*, 6438. (h) Silva, C. C.; Juárez, R.; Marino, T.; Molinari, R.; García, H. *J. Am. Chem. Soc.* **2011**, *133*, 595. (i) Chen, W. T.; Yang, T. T.; Hsu, Y. J. *Chem. Mater.* **2008**, *20*, 7204. (j) Yang, T. T.; Chen, W. T.; Hsu, Y. J.; Wei, K. H.; Lin, T. Y.; Lin, T. W. *J. Phys. Chem. C* **2010**, *114*, 11414. (k) Khon, E.; Mereshchenko, A.; Tarnovsky, A. N.; Acharya, K.; Klinkova, A.; Hewa-Kasakarage, N. N.; Nemitz, I.; Zamkov, M. *Nano Lett.* **2011**, *11*, 1792.

(5) (a) Awazu, K.; Fujimaki, M.; Rockstuhl, C.; Tominaga, J.; Murakami, H.; Ohki, Y.; Yoshida, N.; Watanabe, T. *J. Am. Chem. Soc.* **2008**, *130*, 1676. (b) Mori, K.; Kawashima, M.; Che, M.; Yamashita, H. *Angew. Chem., Int. Ed.* **2010**, *49*, 8598. (c) Thimsen, E.; Le Formal, F.; Grätzel, M.; Warren, S. C. *Nano Lett.* **2011**, *11*, 35. (d) Brown, M. D.; Suteewong, T.; Kumar, R. S. S.; D'Innocenzo, V.; Petrozza, A.; Lee, M. M.; Wiesner, U.; Snaith, H. J. *Nano Lett.* **2011**, *11*, 438. (e) Liu, L. P.; Wang, G. M.; Li, Y.; Li, Y. D.; Zhang, J. Z. *Nano Res.* **2011**, *4*, 249.

(6) Nakato, Y.; Tsubomura, H. *J. Photochem.* **1985**, *29*, 257.

(7) (a) Camden, J. P.; Dieringer, J. A.; Zhao, J.; Van Duyne, R. P. *Acc. Chem. Res.* **2008**, *41*, 1653. (b) Anker, J. N.; Hall, W. P.; Lyandres, O.; Shah, N. C.; Zhao, J.; Van Duyne, R. P. *Nat. Mater.* **2008**, *7*, 442. (c) Ferry, V. E.; Munday, J. N.; Atwater, H. A. *Adv. Mater.* **2010**, *22*, 4794. (d) Li, J. F.; Huang, Y. F.; Ding, Y.; Yang, Z. L.; Li, S. B.; Zhou, X. S.; Fan, F. R.; Zhang, W.; Zhou, Z. Y.; Wu, D. Y.; Ren, B.; Wang, Z. L.; Tian, Z. Q. *Nature* **2010**, *464*, 392.

(8) (a) Park, K.; Vaia, R. A. *Adv. Mater.* **2008**, *20*, 3882. (b) Cardinal, M. F.; Rodriguez-Gonzalez, B.; Alvarez-Puebla, R. A.; Perez-Juste, J.; Liz-Marzan, L. M. *J. Phys. Chem. C* **2010**, *114*, 10417. (c) Becker, J.; Zins, I.; Jakab, A.; Khalavka, Y.; Schubert, O.; Sonnichsen, C. *Nano Lett.* **2008**, *8*, 1719. (d) Lee, Y. H.; Chen, H.; Xu, Q. H.; Wang, J. F. *J. Phys. Chem. C* **2011**, *115*, 7997. (e) Okuno, Y.; Nishioka, K.; Kiya, A.; Nakashima, N.; Ishibashi, A.; Niidome, Y. *Nanoscale* **2010**, *2*, 1489.

(9) (a) Soller, B. J.; Hall, D. G. *J. Opt. Soc. Am. A* **2001**, *18*, 2577. (b) Pala, R. A.; White, J.; Barnard, E.; Liu, J.; Brongersma, M. L. *Adv. Mater.* **2009**, *21*, 3504.